JOURNAL OF MAGNETIC RESONANCE **125,** 193–196 (1997)
ARTICLE NO. MN961093

Pure-Phase Homo- and Heteronuclear *J* Spectra with Tilted Cross Peaks for an Accurate Determination of Coupling Constants

WIKTOR KOŹMIŃSKI,* STEFAN BIENZ, SVETOSLAV BRATOVANOV, AND DANIEL NANZ†

Organisch-chemisches Institut, Universität Zürich, Winterthurerstrasse 190, CH-8057 Zürich, Switzerland

Received December 2, 1996

In a recent publication, we have shown how homonuclear broadband decoupling techniques can be combined with *a*ctive *c*oupling-pattern *t*ilting (ACT) to efficiently measure and assign heteronuclear coupling constants (*1*). In this Communication, we demonstrate the same approaches to allow the acquisition of heteronuclear and homonuclear *J* spectra (*2–5*) with pure phases, tilted cross-peak patterns, and homonuclear I-spin decoupled signals in F_1. Thus, I-spin couplings of interest can be accurately measured irrespective of further homonuclear couplings. As examples, the sequences are shown to yield vicinal silicon–proton couplings and a homonuclear *J*-resolved proton spectrum of a peptide NH region.

The basic pulse sequence for heteronuclear ACT-*J* spectroscopy is displayed in Fig. 1a. The phase cycle employed is listed in Table 1. As in conventional *J*-resolved experiments, the I-spin part of the sequence consists of a $\pi/2$ excitation pulse and a chemical-shift refocusing π pulse placed in the center of the time period between excitation and the beginning of signal detection. In order to refocus homonuclear I-spin coupling evolution in addition to chemical-shift evolution between points *a* and *b*, the π pulse is chosen to act either multiplet selectively or spectral-region selectively (*6*). In the latter case, the spins inverted by the π pulse should not exhibit mutual couplings in order for broadband homonuclear decoupling to be achieved (*7*). In place of the π(I) pulse, a BIRD$_x$ pulse (*8, 9*) will be useful when the heteronuclear couplings of interest all have the same magnitude and are large in comparison with homonuclear I-spin couplings. If the I spins to be inverted do not exhibit homonuclear couplings, e.g., they are isolated methyl groups, the π pulse may also be a hard pulse.

The first t_1 period of the sequence is a dummy evolution period which does not cause a modulation of the signal observed at the beginning of t_2 since both the homonuclear I-spin coupling and the I-spin chemical-shift evolution are refocused at point *b*. During the two delays $\Delta/2$, the I-spin magnetization evolves under the heteronuclear coupling with $\sin(\pi J_{IS}\Delta)$ into antiphase $2I_yS_z$ terms (*10*). Components modulated with $\cos(\pi J_{IS}\Delta)$ are purged by an appropriate cycling of φ_3, φ_4, and the receiver phase (*11, 12*). In the subsequent t_1 period, the spin systems evolve under the heteronuclear coupling interaction. Again, the evolution under the I-spin Zeeman and homonuclear coupling interaction can be neglected because of their refocusing at point *b*. At the end of the t_1 period, the density-matrix components of interest are adequately described by

$$\sigma_b = 2I_yS_z\cos(\pi J_{IS}t_1) - I_x\sin(\pi J_{IS}t_1). \qquad [1]$$

Just prior to acquisition the composite S pulse $\{(\pi/2)_x, (\pi)_{\varphi_5}, \pi(2)_x\}$ either inverts the sign of the antiphase terms ($\varphi_5 = -y$) (*13*) or leaves them unchanged ($\varphi_5 = -x$). By appropriate selection of the receiver phase (or of φ_1), it is thus possible to measure two data sets where either the antiphase cosine terms or the in-phase sine terms are summed up separately (*14*). With respect to their t_1 modulation, these two data sets represent two orthogonal components which allow the generation of pure-phase spectra by the method of States *et al.* (*15*). Due to the phase difference of the two components in t_2, either φ_1 or the receiver phase needs to be incremented by $\pi/2$ for the second data set.

The cosine term in Eq. [1] represents a signal that displays the heteronuclear coupling in-phase in F_1, whereas it is in antiphase in F_2, as represented in Fig. 2a. In contrast, the phase-corrected imaginary part with the sine term represents an antiphase/in-phase signal with respect to F_1 and F_2. Upon combination, an E.COSY-like tilted peak pattern is obtained which displays the active S,I coupling in antiphase in the projections of both dimensions (*1*). Since homonuclear I-spin decoupling is achieved in F_1, this allows an accurate determination of the heteronuclear coupling.

As an example, consider the spectrum displayed in Fig. 3, which was measured with a mixture of the following (E) and (Z) isomers:

* Present address: Department of Chemistry, Warsaw University, ul. Pasteura 1, 02-093 Warsaw, Poland.

† To whom correspondence should be addressed at Universitätsspital Zürich, Departement für Medizinische Radiologie, MR-Zentrum, Rämistrasse 100, 8091 Zürich, Switzerland.

1090-7807/97 $25.00

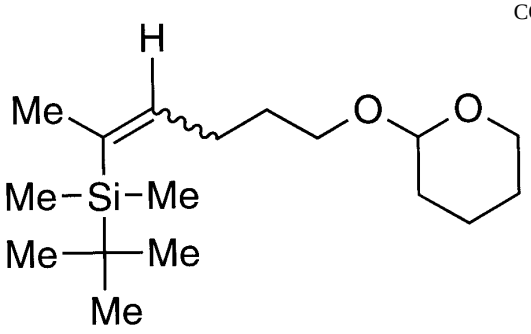

Although even the central signal of each olefinic proton represents at least a quartet × triplet, the only splitting observed in the F_1 dimension of the heteronuclear ACT-J spectrum is caused by the additional heteronuclear coupling of the ^{29}Si isotopomers. Due to the suppression of half of the cross-peak components, accurate values for the heteronuclear coupling can be read from slices extracted either along the F_1 or the F_2 dimension. Note that an exact measurement of the heteronuclear vicinal coupling constants from silicon-detected spectra is not easy and in many cases impossible, since the silicon nucleus is coupled to a large number of protons (*16*). In comparison with such experiments, the sequence presented in Fig. 1a is more sensitive and yields more accurate values in addition to an unambiguous assignment of the I-spin coupling partner. We consider this experiment to be the method of choice for the measurement of a particular heteronuclear coupling of interest. If the X nucleus occurs with 100% abundance, the S-filter part of the sequence, including the $\Delta/2$ delays, as well as the dummy evolution period, except for a compensation of the duration of the S-spin pulses, can be omitted, which considerably simplifies the experiment. Related experiments without active coupling-pattern tilting are described in Ref. (*17*).

Active coupling-pattern tilting involves selective inversion of a coupling partner of the signals of interest. Because of the well-defined and separated spectral regions of NH and H_α resonances in peptide proton spectra, it should be feasible to obtain homonuclear pure-phase ACT-J spectra of the NH region. However, the correctness of the extracted coupling constants will critically depend on how well the α protons can be selectively inverted. A first implementation of such

TABLE 1
Phase Cycling Employed for the Heteronuclear ACT-J Experiment for Rare S Spins Depicted in Fig. 1a

	Real part of t_1 modulation	Imaginary part of t_1 modulation
φ_1	$y, -y$	x, x
φ_2	$8x, 8y, 8(-x), 8(-y)$	
φ_3	$2x, 2(-x)$	
φ_4	$4x, 4(-x)$	
φ_5	$-x, -y$	
$\varphi_{receiver}$	$2x, 4(-x), 2x, 2(-x), 4x, 2(-x)$	

Note. The real and imaginary parts of the t_1 modulation are stored in separate memory locations.

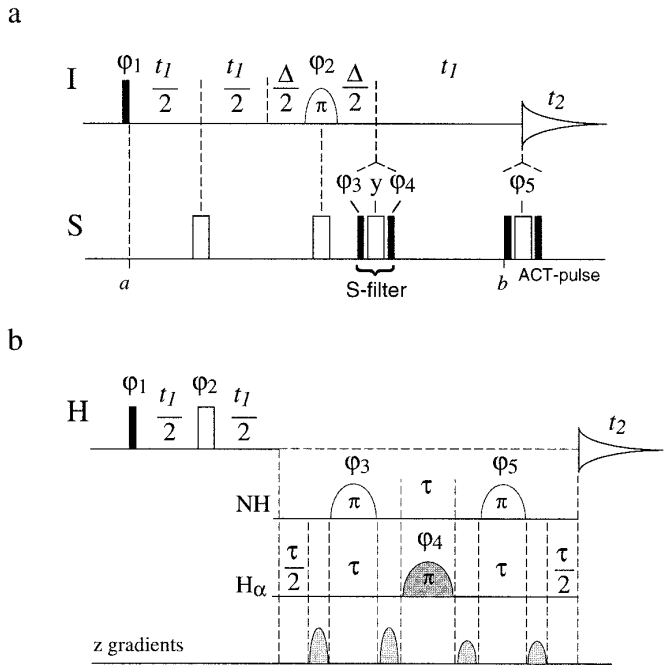

FIG. 1. Suggested heteronuclear (a) and homonuclear (b) ACT-J experiments. Narrow dark and wide unfilled bars represent $\pi/2$ and π pulses, respectively. Multiplet or spectral-region selective π pulses are represented by bell-shaped patterns. $\Delta/2$ in the isotopomer-selection part of sequence (a) is set to $(4J_{SI})^{-1}$. I-spin chemical-shift and homonuclear coupling evolution during all of the S-spin pulses are compensated for by allowing short delays between the two I-spin pulses. In sequence (b), τ corresponds to the duration of the spectral-region selective π pulses. The two field-gradient pulses in each of the first and second pulse pairs are identical; however, they are different for each pair.

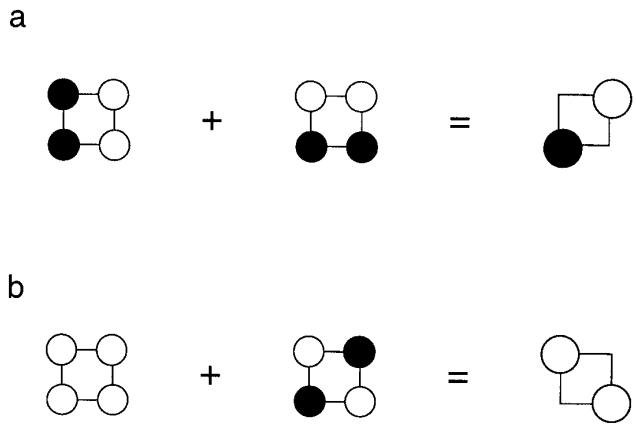

FIG. 2. Active coupling-pattern tilting as employed in this work. Reference (*1*) describes complementary tilting schemes. Scheme (a) was followed in the isotopomer-filtered heteronuclear experiment and scheme (b) in the homonuclear experiment.

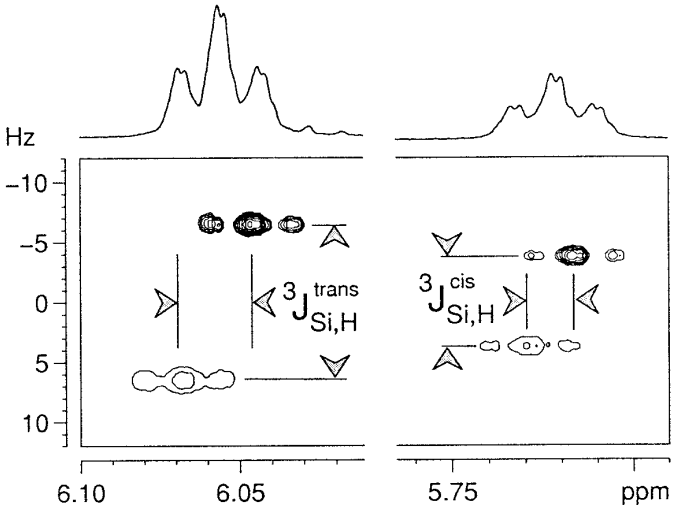

FIG. 3. Heteronuclear (^{29}Si, ^{1}H) ACT-*J* spectrum of an (E)/(Z) mixture of the compound displayed in the text. Proton chemical shifts along F_2 are correlated with heteronuclear couplings along F_1. For negative peaks, only two levels are plotted. As expected, the vicinal coupling across the olefinic bond is larger when the coupling nuclei are in *trans* position (13.0 vs 7.6 Hz). The spectrum was obtained in 1 h from an approximately 0.12 *M* $CDCl_3$ solution (*E* isomer; the *E*/*Z* ratio was approximately 3:2) on a Bruker AMX-600 MHz spectrometer at 300 K, using a 5 mm inverse broadband probe. $\Delta/2$ was set to 25 ms. The spectral-region-selective π pulse to invert the olefinic protons had a 15 ms RE-BURP amplitude-modulation profile (*21*); 32 scans were coherently added for 16 complex points in t_1. The spectral widths were 25 Hz and 2 ppm in F_1 and F_2, respectively. The 1024 × 16 complex data matrix was zero-filled to 8192 × 256 complex points and weighted by exponential windows with a broadening factor of 0.3 and 0.2 Hz in F_1 and F_2 prior to Fourier transformation.

a sequence is displayed in Fig. 1b. In principle, a standard *J*-resolved sequence must only be supplemented with a selective-inversion pulse acting on the α protons just prior to acquisition in half of the experiments. However, this pulse cannot be short enough on the time scale of chemical-shift evolution of the NH protons for its duration to be neglected. Therefore, it is placed in the center of a refocusing excitation-sculpting sequence (*18*) with two gradient-assisted spin echoes (*19, 20*). The phase cycling employed is depicted in Table 2. In this experiment, the real part of the t_1 modulation represents an in-phase/in-phase cross-peak signal as represented in Fig. 2b. In contrast, the imaginary part represents an antiphase/antiphase pattern. Again, the phase of the imaginary part in t_2 must be corrected to obtain a standard complex data set in t_1. In this case, this is achieved by a receiver phase shift of $\pi/2$.

As an example, Fig. 4a displays NH signals of the peptide gramicidin dissolved in DMSO-d_6. Note the tilt and the separation in F_1 of the two doublet components. The splitting of the Phe NH signal is determined to be 3.85 Hz, in contrast to a splitting of 3.49 Hz directly read from the proton 1D spectrum. When lowering the plot levels in the spectrum, the cross-peak components that should be suppressed become also visible in Fig. 4b. This incomplete suppression is mainly attributed to a nonideal inversion of the H_α protons by the selective π pulse. The problem occurred with several different amplitude-modulation envelopes of this pulse. In addition, with our hardware we were not able to obtain satisfying results when working with peptides in 9/1 H_2O/D_2O solutions.

TABLE 2
Phase Cycling of the Homonuclear ACT-*J* Experiment

	Real part of t_1 modulation	Imaginary part of t_1 modulation
φ_1	x, x, y, y	
φ_2	$8y, 8(-x)$	
φ_3	$16x, 16y$	
$\pi(H_\alpha)$ pulse	No, yes	
φ_4	$4x, 4y$	
φ_5	$16(-x), 16(-y)$	
$\varphi_{receiver}$	$2(x, x, -y, -y)$, $2(-x, -x, y, y)$	$2(y, -y, x, -x)$, $2(-y, y, -x, x)$

Note. The selective π pulse on the α protons is applied in every second scan only. The real and imaginary parts of the t_1 modulation are stored in separate memory locations.

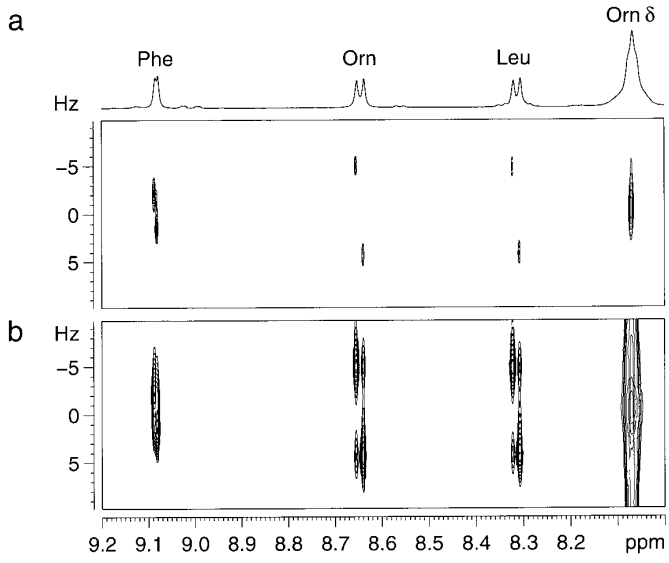

FIG. 4. Part of a homonuclear ACT-*J* spectrum of a 50 m*M* gramicidin S solution in DMSO-d_6. Proton chemical shifts and couplings along F_2 are correlated with homonuclear (NH, H_α) couplings along F_1. The spectrum was measured in 1 h on a Bruker AMX-600 MHz spectrometer at 300 K, using a 5 mm ^{1}H, ^{13}C, ^{15}N triple-resonance probe equipped with an actively shielded *z*-gradient coil. τ was 2 ms. The spectral-region-selective π pulses had a RE-BURP amplitude-modulation profile (*21*) for the pulses acting on NH protons and a Gaussian profile for inversion of the H_α; 32 scans were coherently added for 16 complex points in t_1. The data matrix was zero-filled to 8192 × 128 complex points and weighted with a cosine window in t_2 and an exponential function with a line-broadening factor of 0.5 Hz in t_1 prior to Fourier transformation.

In conclusion, both of the ACT-*J* experiments presented were shown to yield pure-phase and tilted cross peaks. However, improvements will be necessary to make the homonuclear experiment a valuable tool in routine work. In contrast, the heteronuclear experiment presented provides very efficient access to accurate values of heteronuclear coupling constants of I spins that do not mutually couple and can be inverted by a selective π pulse. This sequence can be simplified to measure heteronuclear ACT-*J* spectra in cases with a 100% abundant S spin. On the other hand, pulsed field gradients might be introduced for less abundant S spins. The experiment will be especially useful when the heteronuclear coupling splitting in the I-spin spectrum is obscured by homonuclear couplings among the I spins.

ACKNOWLEDGMENTS

This work was supported by the Swiss National Science Foundation and the Dr. Helmut Legerlotz-Stiftung. We thank W. von Philipsborn for his continuous interest and support and Zoltan Molnar for providing the vinylsilane sample.

Note added in proof. The sensitivity of ACT spectroscopy as presented in this Communication and in HECADE experiments (*1*) can be improved by a factor of $\sqrt{2}$ by acquiring echo and antiecho data sets and processing them accordingly (*22, 23*). In the ACT-*J* spectroscopy, the last composite S pulse would be set to 0 for one data set and to π for the other data set. In HECADE experiments, the gradient echo selection would have to be combined with a 0 degree composite S pulse and the antiecho selection with a composite π pulse, or vice versa.

REFERENCES

1. W. Koźmiński and D. Nanz, *J. Magn. Reson.* **124,** 383 (1997).
2. W. P. Aue, J. Karhan, and R. R. Ernst, *J. Chem. Phys.* **64,** 4226 (1976).
3. G. Bodenhausen, R. Freeman, R. Niedermeyer, and D. L. Turner, *J. Magn. Reson.* **24,** 291 (1976).
4. L. Müller, A. Kumar, and R. R. Ernst, *J. Magn. Reson.* **25,** 383 (1977).
5. K. Nagayama, P. Bachmann, K. Wüthrich, and R. R. Ernst, *J. Magn. Reson.* **31,** 133 (1978).
6. A. Bax, *J. Magn. Reson.* **57,** 314 (1984).
7. V. V. Krishnamurthy, *J. Magn. Reson. A* **121,** 33 (1996).
8. J. R. Garbow, D. P. Weitekamp, and A. Pines, *Chem. Phys. Lett.* **93,** 504 (1982).
9. A. Bax, *J. Magn. Reson.* **53,** 517 (1983).
10. O. W. Sørensen, G. W. Eich, M. H. Levitt, G. Bodenhausen, and R. R. Ernst, *Prog. NMR Spectrosc.* **16,** 163 (1983).
11. L. Müller, *J. Am. Chem. Soc.* **101,** 4481 (1979).
12. O. Zerbe, J. H. Welsh, J. A. Robinson, and W. von Philipsborn, *J. Magn. Reson.* **100,** 329 (1992).
13. M. H. Levitt and R. Freeman, *J. Magn. Reson.* **33,** 473 (1980).
14. P. Bachmann, W. P. Aue, L. Müller, and R. R. Ernst, *J. Magn. Reson.* **28,** 29 (1977).
15. D. J. States, R. A. Haberkorn, and D. J. Ruben, *J. Magn. Reson.* **48,** 286 (1982).
16. R. Rossi, A. Carpita, F. Bellina, and M. DeSantis, *Gazz. Chim. Ital.* **121,** 261 (1991).
17. M. Liu, R. D. Farrant, J. M. Gillam, J. K. Nicholson, and J. C. Lindon, *J. Magn. Reson. B* **109,** 275 (1995).
18. T.-L. Hwang and A. J. Shaka, *J. Magn. Reson. A* **112,** 275 (1995).
19. E. L. Hahn, *Phys. Rev.* **80,** 580 (1950).
20. R. E. Hurd, *J. Magn. Reson.* **87,** 422 (1990).
21. H. Geen and R. Freeman, *J. Magn. Reson.* **93,** 93 (1991).
22. J. Boyd, N. Soffe, B. John, D. Plant, and R. Hurd, *J. Magn. Reson.* **98,** 660 (1992).
23. J. R. Tolman, J. Chung, and J. H. Prestegard, *J. Magn. Reson.* **98,** 462 (1992).